J. Micromech. Microeng. **7** (1997) 316–322. Printed in the UK PII: S0960-1317(97)83314-1

Experimental analysis on the anodic bonding with an evaporated glass layer

Woo-Beom Choi†, Byeong-Kwon Ju†, Yun-Hi Lee†, Jee-Won Jeong†, M R Haskard‡, Nam-Yang Lee§, Man-Young Sung‖ and Myung-Hwan Oh†

† Division of Electronics and Information Technology, Korea Institute of Science and Technology, 130-650, PO Box 131, Cheongryang, Seoul, Korea
‡ Microelectronics Centre, University of South Australia, SA, 5098, Australia
§ Information Display Research Institute, Orion Electric Co., Suwon, Korea
‖ Department of Electrical Engineering, Korea University, Seoul, Korea

Received 10 April 1997, accepted for publication 2 September 1997

Abstract. We performed a silicon-to-silicon anodic bonding process using a glass layer deposited by electron beam evaporation. Corning No 7740 Pyrex glass was used as the source material of electron evaporation. The effects on the bonding process were investigated as a function of the thickness of the glass layer and the concentration of sodium ions in the glass layer. The surface roughness of the glass layer decreased with increasing thickness of the glass layer. It was observed that the deposited glass layers of more than 1.5 μm thickness had very small surface roughness. The depth profile of sodium ions showed that the glass layer deposited by electron beam evaporation contained many more sodium ions than the glass layer deposited by sputtering. The silicon-to-silicon bonding process was performed at temperatures in the range of 135–240 °C with an electrostatic voltage in the range of 35–100 V_{DC}. A pull test revealed that the tensile strength of bonded specimens was in the region of 1–8 MPa. The role of sodium ions in anodic bonding was studied by investigating the theoretical bonding mechanism and examining the results of secondary-ion mass spectroscopy (SIMS) analysis on the glass layer before and after the bonding process.

1. Introduction

Anodic bonding has become one of the important technologies in the fabrication of micromachining devices with many advantages, such as solid-state bonding, a bonding process without the requirement of either a post-heat-treatment at high temperature [1–3] or hydrophilic cleaning [4, 5] which can bring degradation of device lifetime [6]. Anodic bonding has been concentrated on silicon-to-silicon bonding since the anodic bonding method using a sputtered Pyrex glass layer was invented by Brooks and Donovan in 1972 [7–11]. Pyrex glass has been commonly used for this method because it has approximately the same thermal expansion coefficient as silicon and Pyrex glass contains metallic atoms which are necessary in anodic bonding, but unfortunately the sputtering of the glass layer has the disadvantages of very low deposition rate and different compositions compared with the glass target [12].

Pyrex glass contains metallic atoms such as sodium or lithium. Corning No 7740 glass contains sodium and is the most popular material used in anodic bonding, since the process was invented by Wallis and Pomerantz in 1969 [13]. Sodium plays a very important role in the field assisted silicon-to-silicon bonding a using glass thin-film interlayer or in the silicon-to-Pyrex glass plate bonding. The sodium can be easily ionized at room temperature

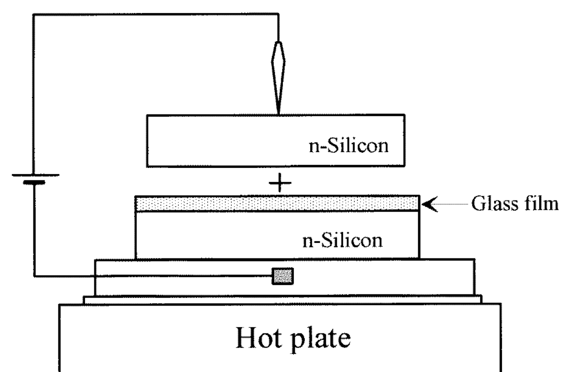

Figure 1. The experimental set-up for silicon-to-silicon anodic bonding.

0960-1317/97/040316+07$19.50 © 1997 IOP Publishing Ltd

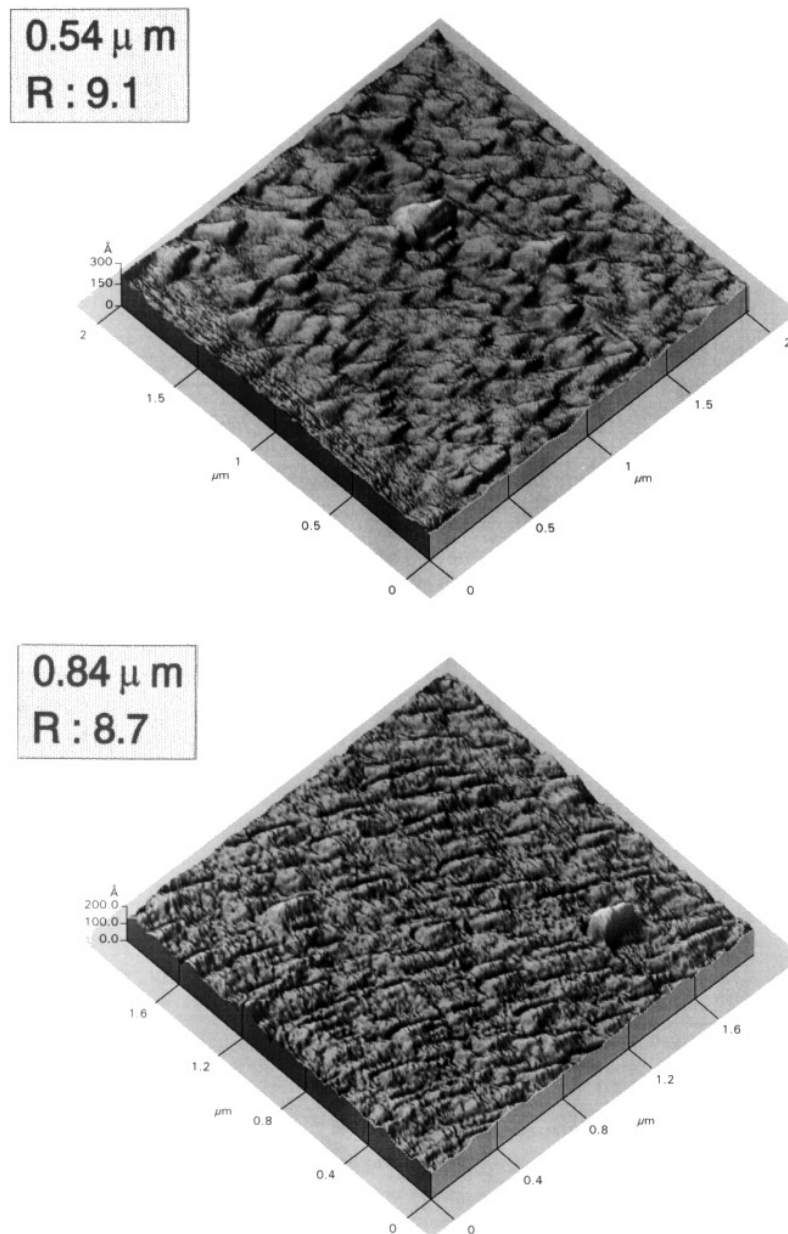

Figure 2. An AFM image of the glass layer deposited by electron beam evaporation (0.54, 0.84, 1.10, 1.54 μm). *R* denotes the average roughness of the glass layer [Å].

and the positive sodium ions in the glass layer become quite mobile at elevated temperature [14, 15]. When a d.c. voltage is applied across the silicon–glass layer–silicon sandwich, the positive sodium ions in the deposited glass layer are transported toward the cathode silicon by the applied negative voltage. A sodium depleted layer is formed at the surface region of the deposited glass layer, leaving fixed negative ions (oxygen ions) in the glass layer adjacent to the bare silicon to be bonded. As a result, a space charge region is formed at the interface between the surfaces of the glass layer and the bare silicon to be bonded. The resulting large electrostatic force pulls them together, allowing the formation of atomic bonds.

In this work, we performed silicon-to-silicon anodic bonding under low temperature and low voltage using a Pyrex glass layer deposited by electron beam evaporation, having a high deposition rate and resulting in very small surface roughness and containing many more sodium ions in the glass layer deposited by electron beam evaporation than one deposited by sputtering. Anodic bonding using the glass layer deposited by electron beam evaporation could be performed at lower temperature and voltage in the bonding process than that using the glass layer deposited by sputtering. We furthermore investigated the role of sodium ions for silicon-to-silicon anodic bonding with reference to the theoretical bonding mechanism as well as the results of secondary-ion mass spectroscopy (SIMS) analysis.

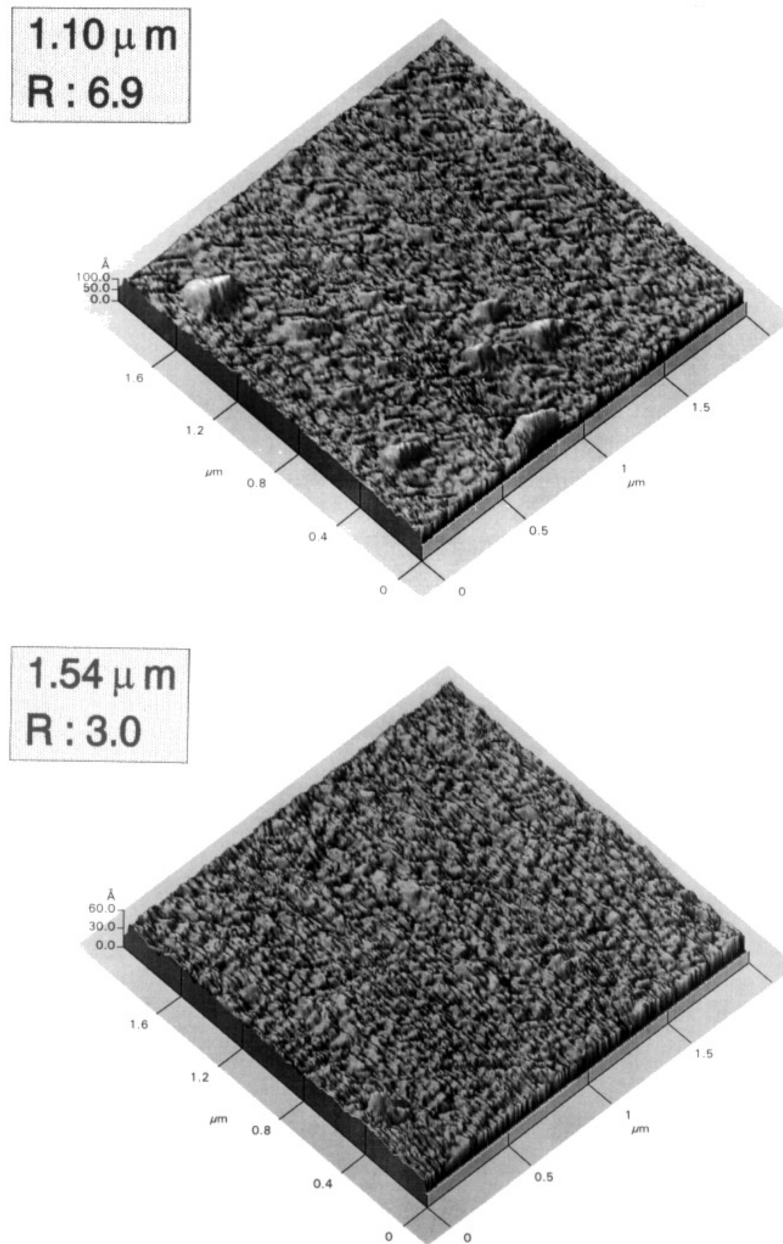

Figure 2. (Continued)

2. Experimental details

Pyrex glass layers were deposited on (100) n-type 4 in silicon wafers by electron beam evaporation at a substrate temperature of 230 °C. The process chamber was evacuated by a diffusion pump down to 2×10^{-5} Torr. The vacuum was about 5×10^{-5} Torr during the evaporation. Corning No 7740 glass was used as the source material of electron beam evaporation. The deposition rate of the glass layer was varied between 5 Å s^{-1} and 50 Å s^{-1}. The effect on the dielectric strength of the glass layer was investigated as a function of the deposition rate. The deposited glass layers with thickness ranging from 0.4 to 2 μm were used for this work. To study the effect of the thickness on the surface roughness, the surface morphology was observed by the atomic force microscope (AFM). The compositions of the glass layer deposited by electron beam evaporation were compared with those of the glass layer deposited by sputtering, using SIMS analysis.

Both silicon with the deposited glass layer and bare silicon were cleaned by two-step cleaning before the bonding process. The specimens were ultrasonically cleaned for 5 min in acetone followed by deionized water rinsing and then the specimens were ultrasonically cleaned for 5 min in methanol again. After a final rinse in deionized water, the cleaned specimens were dried by a nitrogen gun and heated for 20 min at 150 °C. The assemblies were placed on specially designed field assisted bonding

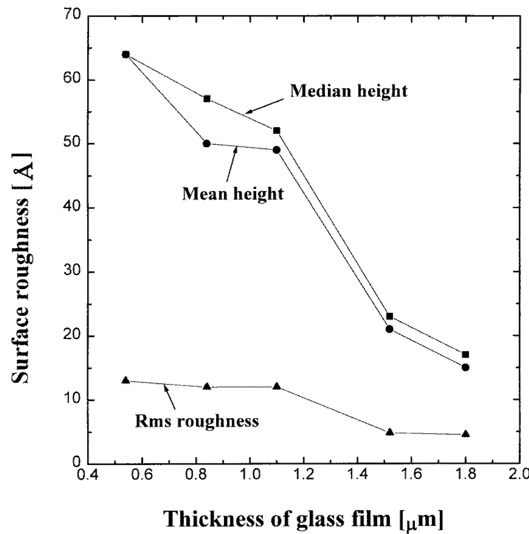

Figure 3. The surface roughness of the glass layers with different thicknesses.

equipment (figure 1). Without applying an external force the bonding process was performed at temperatures in the range of 135–240 °C with an electrostatic voltage in the range of 35–100 V_{DC} using a point electrode. A negative voltage was applied to the silicon wafer with the deposited glass layer for 10 min, and the bonding current was recorded under normal atmosphere.

3. Results and discussion

The surface roughness of the deposited glass layer is one of the most important parameters in anodic bonding. One of the significant effects of the rough surface is decrease of the bonding strength or even failure of bonding [12]. Figure 2 shows an AFM image of the surface of the deposited glass layers with different thicknesses. With increasing thickness of the glass layer, the surface roughness of the glass layer decreased and then remained at a minimized level (figure 3). It was observed that the deposited glass layers of more than 1.5 μm thickness had very small surface roughness. Experimental results revealed that the glass layer of less than 1 μm thickness was not suitable for the bonding process.

In order to compare the composition of the glass layer deposited by electron beam evaporation with that of the bulk glass plate and the glass layer deposited by sputtering, SIMS analysis was performed on the three types of specimen. The depth profiles of the three types of specimen, which were obtained by SIMS using cesium ions (Cs^{+}) incident on the surface of the bulk glass and the deposited glass layer, causing positive secondary ions to be ejected, are shown in figure 4. The results shown in figure 4 were collected at the same sputtering rate of about 10 nm min^{-1}. It was confirmed that the sodium concentration of the bulk glass plate is nearly the same as that of the glass layer deposited by e-beam, whereas the glass layer deposited by sputtering has far fewer sodium ions than the bulk glass. The glass layer deposited by electron beam evaporation contained more sodium ions than the glass layer deposited by sputtering. Therefore, it is concluded that this high concentration of Na contributed to the lowering bonding temperature as well as applied voltage.

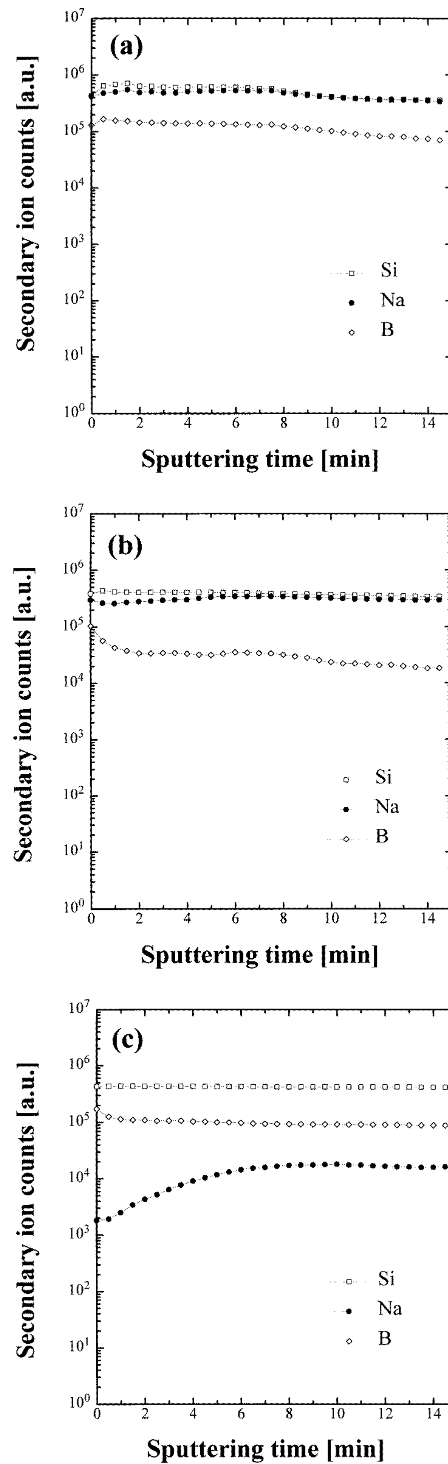

Figure 4. SIMS depth profiles in the surface region of (a) the bulk glass, (b) the glass layer deposited by electron beam evaporation, and (c) the glass layer deposited by sputtering.

In order to investigate the variation of the dielectric strength of the glass layer as a function of the deposition rate, Al electrode (diameter 0.6 mm) was formed by thermal

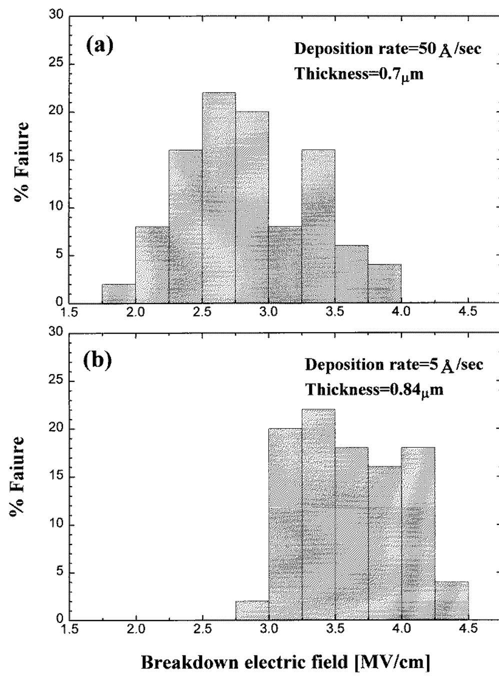

Figure 5. The dielectric breakdown histograms of the glass layer deposited at (a) 50 Å s^{-1} deposition rate and (b) 5 Å s^{-1} deposition rate.

evaporation on the top of the e-beam evaporated glass layer. At the 5 Å s^{-1} deposition rate, the distribution of breakdown fields measured by the time-zero dielectric breakdown (TZDB) technique was higher than that for 50 Å s^{-1} deposition rate as shown in figure 5. With the specimens deposited at the 5 Å s^{-1} rate, silicon-to-silicon bonding could be performed at higher temperature and higher voltage than using the specimens deposited at the 50 Å s^{-1} rate without dielectric breakdown during the bonding process.

The role of sodium ions in anodic bonding is most easily studied by observing change of the Na depth profiles before and after the bonding process. Figure 6(a) shows that the sodium ion counts at the surface region of the deposited glass layer was greatly reduced after bonding, as compared with figure 4(b) which is the depth profile of the glass layer before the bonding process. The sodium ions were almost depleted from the surface region of the deposited glass layer in contact with the bare silicon to be bonded. This agrees with the suggested theoretical model. The sputtering rate of the SIMS was about 10 nm min^{-1}. The sodium ions that are depleted from the surface region of the glass layer accumulate at the back-side region of the deposited glass layer and are neutralized there.

The bonded samples were pulled in order to measure the bond strength. When the pull tests were performed, it was observed that the deposited glass layers were partly or totally removed from the silicon on which they were originally deposited and were found on the surface of the silicon to be bonded. Results of SIMS analysis on the totally removed deposited glass layer indicate that the sodium ions accumulate at the back-side region of the deposited glass layer. Figure 6(b) shows that the sodium ions are accumulated at the back side and decrease abruptly from the back side to the bulk region of the deposited glass layer.

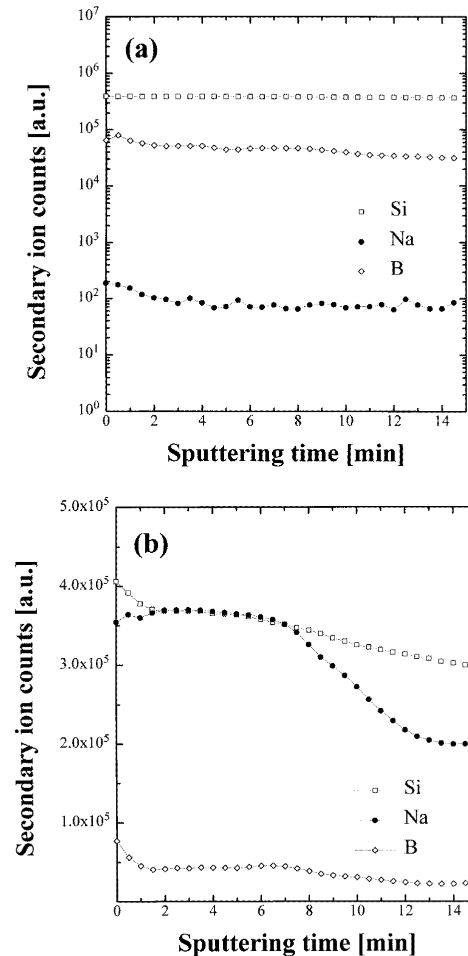

Figure 6. SIMS depth profiles of the glass layer in (a) the surface region after the bonding process and (b) the back-side region after the bonding process.

In order to characterize the bonding process, current–time characteristics were measured during the start period. The bonding current was measured at a temperature in the range of 135–145 °C with an applied electrostatic voltage of 55 V_{DC} for 10 min. The bonding current decayed rapidly and then remained at a minimized level, as presented in figure 7. The obtained current density profile was well fitted with a typical current–time relationship for anodic bonding process. As a result, it is easy to understand that the observed current during the bonding process can be attributed to the transport of the sodium ions in the glass layer and an increase in bonding temperature results in a higher diffusion rate of the sodium ions, which in turn causes a higher bonding current.

To explain the threshold temperature for the bonding process, we examined the capacitance of the glass layer as a function of temperature. Figure 8 shows the temperature dependence of the capacitance for the glass layer. The capacitance increased rapidly at the temperature of about 135 °C. The rapid increase of capacitance may be attributed

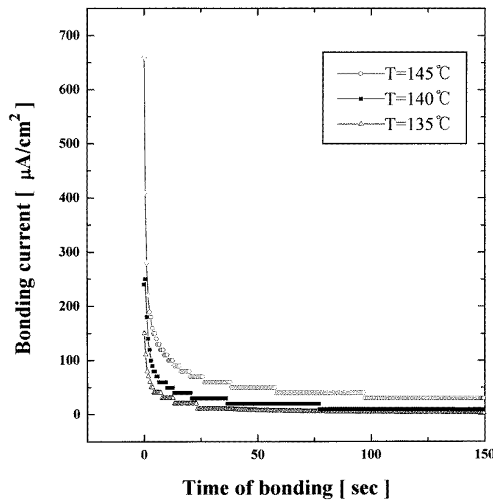

Figure 7. Dependence of the bonding current on temperature during the initial bonding stage.

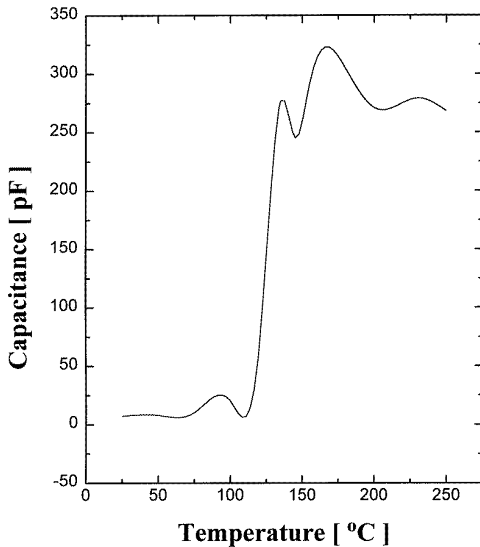

Figure 8. Temperature dependence of capacitance for the glass layer deposited by electron beam evaporation.

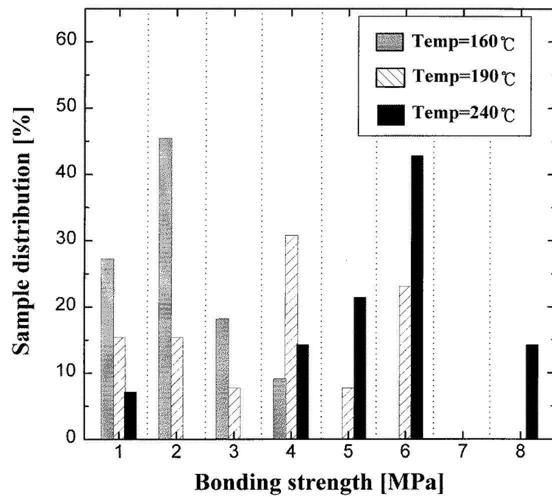

Figure 9. The bonding strength histogram.

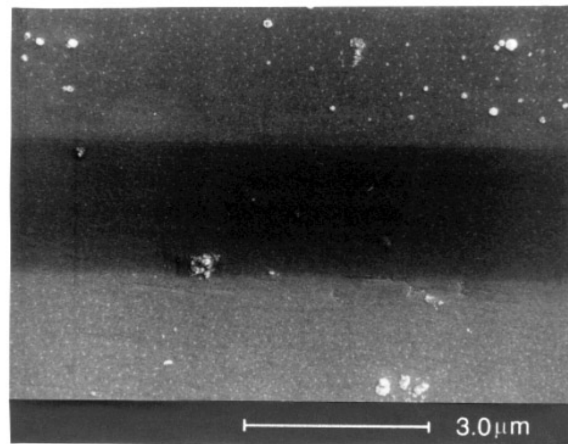

Figure 10. An SEM photograph of the bonded interface region after polishing.

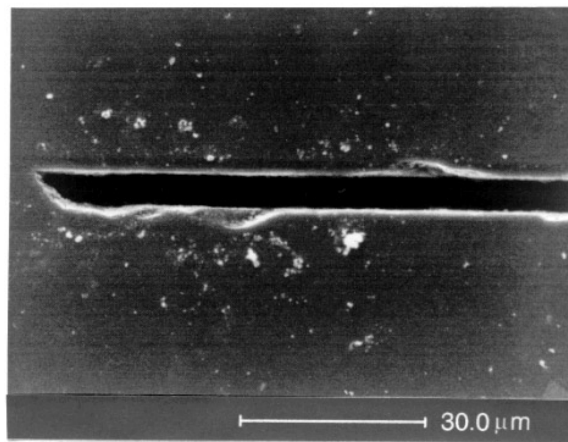

Figure 11. An SEM photograph of the cavity sealed by anodic bonding.

to the ionization of sodium as well as the movement of sodium ions. Hence, it can be clearly understood that the bonding is initiated at a temperature of about 135 °C, accompanying the increase of capacitance.

To evaluate the tensile strength of the bonded specimens, a pull test was used. The experimental results obtained are illustrated in figure 9. The bonding strength is plotted as a function of the bonding temperature for the specimens bonded at 100 V_{DC}. With increasing bonding temperature, the bonding strength increased.

After determining the bonding strength distribution, the bonded samples were cut and polished to observe the bonded interface region of the silicon-to-silicon assembly. Figure 10 shows the cross sectional photograph of silicon–glass layer–silicon to be bonded.

The cavity of 15 mm × 15 mm × 8 μm was formed on the silicon substrate by the anisotropic etching of the silicon substrate in ethylenediamine–pyrocatechol–water (EPW). Using our anodic bonding process, the cavity was sealed by the silicon with the deposited glass layer (figure 11). The bonded 4 in wafer sets were inspected by infrared camera

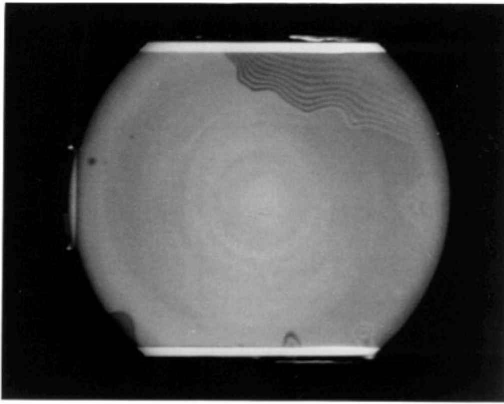

Figure 12. An infrared photograph of the silicon-to-silicon bonded specimen.

(Hamamatsu void inspection system C6145) to investigate the interface fringe. Figure 12 shows the radial spreading of the bonding and the dark fringe of the unbonded region. Based on the fact that the anodic bonding process starts at a point electrode and spread radially [16], the same explanations hold for explaining the observed patterns.

4. Conclusions

In order to realize the silicon-to-silicon anodic bonding process at low voltage and low temperature, we employed a Pyrex glass layer deposited by electron beam evaporation. As the thickness of the glass layer increased, the surface roughness of the deposited glass layer decreased. The glass layer deposited by electron beam evaporation contained many more sodium ions than the one deposited by sputtering. The silicon-to-silicon anodic bonding phenomenon was investigated at a temperature of 135 with an applied voltage of 35 V_{DC}. The obtained results can be utilized to vacuum packaging of microelectronic devices and microsensors. From SIMS analysis on the glass layer before and after the bonding process, the role of the sodium ions in the anodic bonding mechanism was investigated.

Acknowledgment

This work was supported by the Ministry of Trade, Industry and Energy in Korea.

References

[1] Maszara W P 1991 Silicon-on-insulator by wafer bonding *J. Electrochem. Soc.* **138** 341–7
[2] Okabayshi O, Shirotori H, Sakurazawa H and Kanda E 1990 Evaluation of directly bonded silicon wafer interface by the magic mirror method *J. Cryst. Growth* **103** 456–60
[3] Ling L and Shimura F 1992 Relationship between interfacial native oxide thickness and bonding temperature in directly bonded silicon wafer pairs *J. Appl. Phys.* **71** 1237–41
[4] Ju B K and Oh M H 1994 Fabrication of silicon membrane using fusion bonding and two-step electrochemical etch-stopping *J. Mater. Sci.* **29** 664–8
[5] Ju B K, Lee Y H, Tchah K H and Oh M H 1995 On the anistropically etched bonding interface of directly bonded (100) silicon wafer pairs *J. Electrochem. Soc.* **142** 547–53
[6] Roberds B E and Farrens S N 1993 Low temperature silicon direct bonding *Electrochem. Soc. Proc.* **93** 240–4
[7] Brooks A A and Donovan R P 1972 Low-temperature electrostatic silicon-to-silicon seals using sputtered borosilicate glass *J. Electrochem. Soc.* **119** 545–6
[8] Hanneborg A, Nese M and Ohlckers P 1991 Silicon-to-silicon anodic bonding with a borosilicate glass layer *J. Micromech. Microeng.* **1** 139–44
[9] Nese M and Hanneberg A 1993 Anodic bonding of silicon to silicon wafers coated with aluminium, silicon oxide, polysilicon or silicon nitride *Sensors Actuators* A **37/38** 61–7
[10] Berenschot J W, Gardeniers J G E, Lammerink T S J and Elwenspork M 1994 New applications of r.f.-sputtered glass films as protection and bonding layers in silicon micromaching *Sensors Actuators* A **41/42** 338–43
[11] Krause P, Sporys M and Obermeier E 1995 Silicon to silicon anodic bonding using evaporated glass *Proc. 8th Int. Conf. Solid-State Sensors and Actuators, Eurosensors IX (Stockholm, Sweden)* vol 1 (Stockholm: Foundation for Sensors and Actuator Technology) pp 228–31
[12] Ko W H, Suminto J T and Yeh G J 1995 Bonding techniques for microsensors *Micromachining and Micropackaging of Transistors* (Amsterdam: Elsevier) pp 41–61
[13] Wallis G and Pomerantz D I 1969 Field assisted glass–metal sealing *J. Appl. Phys.* **40** 3946–9
[14] Kanda Y, Matsuda K and Murayama C 1990 The mechanism of field-assisted silicon-glass bonding *Sensors Actuators* A **21/23** 939–43
[15] Lee W Y, Sequeda F and Salem J 1987 Field-assisted bonding below 200 °C using metal and glass thin-film interlayer *Appl. Phys. Lett.* **50** 522–4
[16] Obermeier E 1995 Anodic wafer bonding *Electrochem. Soc. Proc.* **95/97** 213–20